SCIENCE CHINA
Earth Sciences

•RESEARCH PAPER•

https://doi.org/10.1007/s11430-019-9590-0

Constraints on the Ediacaran-Cambrian boundary in deep-water realm in South China: Evidence from zircon CA-ID-TIMS U-Pb ages from the topmost Liuchapo Formation

Wei WANG[1,2,3], Mingzhong ZHOU[4*], Zhuyin CHU[1,3†], Junjie XU[1,3,5], Chaofeng LI[1,3], Taiyi LUO[6] & Jinghui GUO[1,3]

[1] *State Key Laboratory of Lithospheric Evolution, Institute of Geology and Geophysics, Chinese Academy of Sciences, Beijing 100029, China;*
[2] *University of Chinese Academy of Sciences, Beijing 100049, China;*
[3] *Innovation Academy for Earth Science, Chinese Academy of Sciences, Beijing 100029, China;*
[4] *School of Geographical and Environmental Sciences, Guizhou Normal University, Guiyang 550001, China;*
[5] *China University of Geosciences, Beijing 100083, China;*
[6] *State Key Laboratory of Ore Deposit Geochemistry, Institute of Geochemistry, Chinese Academy of Sciences, Guiyang 550002, China*

Received September 23, 2019; revised January 19, 2020; accepted February 20, 2020; published online March 30, 2020

Abstract The placement of the Ediacaran-Cambrian boundary in deep-water realm in South China and the high-precision temporal framework for the Ediacaran-Cambrian transition in this region have not yet been completely solved. Recently, we have found two K-bentonite beds in the top of the Liuchapo Formation at the Pingyin section, Guizhou Province. It provides an opportunity for constructing the temporal framework of the transitional strata on the Yangtze Platform in South China and for determining the Ediacaran-Cambrian boundary in this area. In this study, we conducted high-precision CA-ID-TIMS U-Pb dating on zircons from the two K-bentonites. The ages of the two K-bentonites were precisely constrained at 536.40±0.47/1.1/1.2 Ma (2σ, n=7, MSWD=0.92) and 541.48±0.46/1.1/1.2 Ma (2σ, n=8, MSWD=1.3). Combining the geochronological results with organic carbon isotope data of chert in the topmost Liuchapo Formation from the section, we suggest that the Ediacaran-Cambrian boundary should be consistent with a significant negative organic carbon isotope excursion between the two K-bentonites. The scheme of the Ediacaran-Cambrian boundary in this study is of great significance for global correlation, and further for unravelling the information of the terminal Ediacaran-early Cambrian ocean.

Keywords Liuchapo Formation, Yangtze Platform, Ediacaran-Cambrian, CA-ID-TIMS, Organic carbon isotope

Citation: Wang W, Zhou M, Chu Z, Xu J, Li C, Luo T, Guo J. 2020. Constraints on the Ediacaran-Cambrian boundary in deep-water realm in South China: Evidence from zircon CA-ID-TIMS U-Pb ages from the topmost Liuchapo Formation. Science China Earth Sciences, 63, https://doi.org/10.1007/s11430-019-9590-0

1. Introduction

The Ediacaran-Cambrian transition, as one of the most significant periods in the history of Earth's evolution, produced a series of global geological, environmental and biological events. For example, the assembly of the Gondwana supercontinent (ca. 580–520 Ma) (Li et al., 2008; Cawood et al., 2013; Yao et al., 2014), origin and radiation of metazoans (Erwin et al., 2011), significant fluctuations in global ocean-atmosphere chemical composition (Canfield et al., 2008; Shields-Zhou and Zhu, 2013), extinction of Ediacaran organisms and diversification of Cambrian organisms (Zhu et al., 2009; Zhu et al., 2019; Zhou et al., 2019). It can be seen that the strata in this special geological period are of great significance for studying global environmental changes, life

* Corresponding author (email: mingzhongzhou@126.com)
† Corresponding author (email: zhychu@mail.igcas.ac.cn)

evolution and other scientific issues. In recent years, it has been the focus of earth science research.

On the Yangtze Platform in South China, one of the best Ediacaran-Cambrian transitional strata in the world and continuous Ediacaran-Cambrian sections have been saved, and the complete marine carbon isotope and fossil information have been documented. This provides an ideal place for studying the evolution of marine environment during the Ediacaran-Cambrian transition period (Zhou et al., 2013; Wang et al., 2014; Zhu et al., 2003; Zhu et al., 2019). In recent years, geologists have made some important achievements in paleontology, stratigraphy and geochemistry of the Ediacaran-Cambrian transitional strata. As a result, a complete framework of carbon isotope stratigraphy and biostratigraphy has been established. However, the research of high-precision geochronology is obviously lagging behind and accurate age data is still lacking. In particular, the Ediacaran-Cambrian boundary in the deep-water area has not yet been determined (Zhou et al., 2013), which limits the precise inter-continental correlation of strata and makes our interpretation of the palaeo-ocean changes uncertain (Wille et al., 2008; Jiang et al., 2007, 2009; Zhu et al., 2019).

We found two K-bentonite beds in the top of the Liuchapo Formation at the Pingyin section in Guizhou Province and conducted a high-precision dating using zircon CA-ID-TIMS U-Pb technique. At the same time, the organic carbon isotope analysis of the chert in the top of the Liuchapo Formation was carried out. Combining the high-precision zircon U-Pb ages of two K-bentonites with organic carbon isotope data of the chert, we proposed that the Ediacaran-Cambrian boundary in deep-water area of the Yangtze Platform in South China shoud be palaced at the horizon (between the two K-bentonites) with a significant negative organic carbon isotope excursion with the top of the Liuchapo Formation. The conclusion implies that the top of the Liuchapo Formation and its equivalents have important correlation value for understanding the global palaeo-ocean change near the Ediacaran-Cambrian boundary.

2. Geological background

During the Ediacaran-Cambrian transition period, South China gradually evolved from a rift basin to a passive continental margin and the Yangtze Platform was in a passive continental marginal environment (Zhu et al., 2003). During this period, the seawater depth in different regions of the Yangtze Platform in South China varied, showing a general trend of deepening from northwest to southeast. Therefore, the Ediacaran-Cambrian transition in this region have facies variance in different regions. From northwest to southeast, the shallow-water platform facies turns to deep-water slope-basin facies (Figure 1). The platform facies mainly developed carbonate and phosphorite strata, while the slope and basin facies mainly produced chert and siliceous carbonaceous shale strata.

Ediacaran-Cambrian sequences in the deep-water slope and basin zone of the Yangtze Platform are continuous. The strata in this region include, in ascending order, the Doushantuo, Liuchapo (or Laobao) and Niutitang formations. The

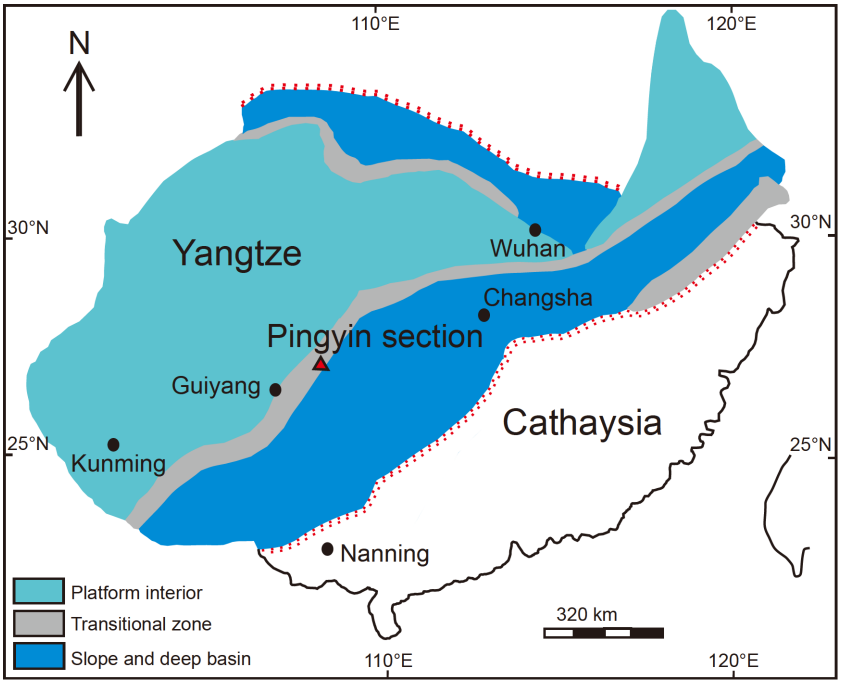

Figure 1 Sketch paleogeographic map of the Yangtze Platform in South China during the Ediacaran-Cambrian period. According to Zhu et al. (2003).

lower part of the Doushantuo Formation is mainly composed of dolomite, while the upper is mainly black shale and the Wenghui biota is preserved in this horizon. The Liuchapo Formation is dominantly consisted of grayish black cherts. The thickness of the chert beds become thinner upward and black shale intercalations occur in the uppermost part of the formation. The Niutitang Formation overlies the Liuchapo Formation and its lower boundary is often marked by a 0.1–0.5 m thick phosphorite layer. The strata above the phosphorite are mainly black shales (Zhou et al., 2013; Lan et al., 2017). The Ni-Mo layer, which is widely distributed on the Yangtze Platform and can be used as a marker for regional correlation, is located at the bottom of the Niutitang Formation (Zhu et al., 2003).

The Pingyin section is located about 2 km east of Taoying Town, Jiangkou County, Guizhou Province. Palaeogeographically, this section is located in the slope zone of the deep-water area on the southeast edge of the Yangtze Platform. The strata exposed at this section, are 4.5 m sequences of the top of the Liuchapo Formation and the overlying Niutitang Formation. We found two grayish white K-bentonites with a thickness of 2 and 15 cm at about 1.2 and 2.4 m, respectively, below the the Liuchapo-Niutitang boundary in this section (Figure 2).

3. Sample collection and processing

We collected two K-bentonite samples at 1.2 and 2.4 m below the boundary between the Liuchapo and Niutitang formations at the Pingyin section. The sample numbers are PY-LB and PY-13, respectively. We strictly avoided contamination of samples by surrounding rocks when sampling. Meanwhile, cherts in the top of the Liuchapo Formation were sampled. The spacing of the chert samples was 0.05 m near the K-bentonites and was 0.2 m for the other parts. A total of 28 samples of fresh chert were collected.

Zircons were separated from K-bentonite samples through conventional heavy liquid and magnetic methods. Finally, we selected over 500 and 1000 zircons from the young and older K-bentonite samples, respectively, under a binocular. Part of the zircons were randomly cast in epoxy mounts and polished until the zircon interior was exposed. Reflected, transmitted light and cathodoluminescence (CL) images of the zircons were taken as in Figure 3. We observed the zircon morphology, and zircons without inclusions and cracks were selected for CA-ID-TIMS U-Pb dating. Chert samples were crushed to 200–400 mesh for analysis of organic carbon isotope composition.

4. Analytical methods

4.1 CA-ID-TIMS U-Pb analysis of zircon

The zircon CA-ID-TIMS experiment was conducted at the Institute of Geology and Geophysics, Chinese Academy of Sciences. Mass spectrometry was performed on a TRITON Plus mass spectrometer.

4.1.1 Dissolution and chemical separation of zircon

A standard CA-ID-TIMS (Chemical Abrasion, CA) method (Mattinson, 2005) was used for the zircon U-Pb analysis. The detailed procedure can be found in the literature (Chu et al., 2016). Zircons were selected under the binoculars and placed in a muffle furnace, and annealed at 900°C for 60 hours to heal the radioactive damage. After quenching, the zircons were leached in 29 mol L^{-1} hydrofluoric acid (HF) inside high-pressure Parr vessels at 180°C for 12 h to partially dissolve the zircon, to remove the region in the zircon suffering from lead loss. Zircons were then fluxed/washed for several hours (at 120°C and in an ultra-sonic bath) in 30% HNO_3, 6 mol L^{-1} HCl and Milli-Q water alternately. Subsequently, zircons were spiked with an appropriated amounts of the mixed ^{205}Pb-^{235}U spike and then completely dissolved in 120 μL 29 mol L^{-1} HF with a trace of 4 mol L^{-1} HNO_3 at 220°C for 48 hours. After this step, the samples were dried to salts, and re-dissolved in 120 μL 6 mol L^{-1} HCl at 180°C overnight. After conversion of the zircon solution to

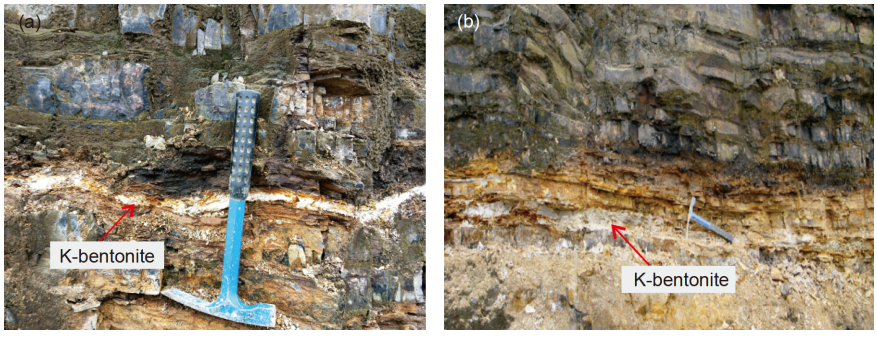

Figure 2 Field photos of two K-bentonites in the top of the Liuchapo Formation at the Pingyin section, South China. (a) K-bentonite at 1.2 m below the upper boundary of the Liuchapo Formation; (b) K-bentonite at 2.4 m below the upper boundary of the Liuchapo Formation; geological hammer handle length in (a) and (b) is 27 cm.

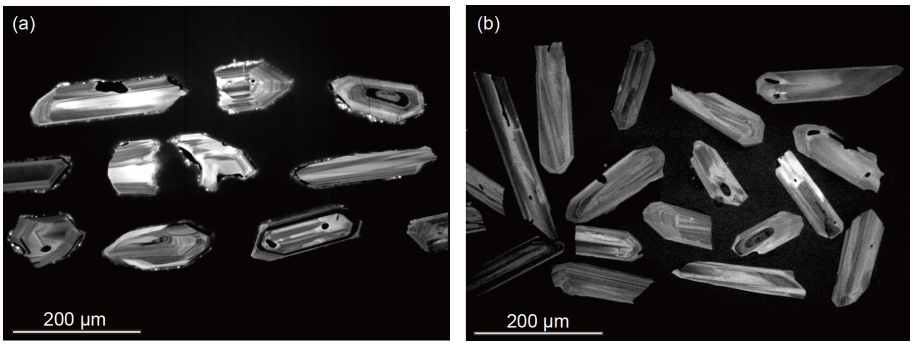

Figure 3 Cathodoluminescence images of zircons from the two K-bentonites in the top of the Liuchapo Formation at the Pingyin section, South China. (a) Zircons from K-bentonite at 1.2 m below the upper boundary of the Liuchapo Formation; (b) zircons from K-bentonite at 2.4 m below the upper boundary of the Liuchapo Formation.

3 mol L^{-1} HCl, Pb and U were separated by anion exchange (AG1-X8, 200–400 mesh) chromatography in 50 μL Teflon FEP micro-columns. The Pb and U were collected in the same Teflon beaker. Finally, 10 μL 0.0375 mol L^{-1} H_3PO_4 was added to the sample solution and dried to dryness, and then ready for mass spectrometric measurements.

4.1.2 Mass spectrometry

The samples were loaded on high purity Re single filaments (0.77 mm wide and 0.038 mm thick; purity: 99.999%) with a silica-gel (Gerstenberger and Haase, 1997) as an ion emitter. A TRITON Plus thermal ionization mass spectrometer were used for Pb and U isotope measurements. A secondary electron multiplier (SEM) was used to determine Pb and U isotopes. Dead time of the SEM was set to 16 ns.

(1) Pb isotope determination. Firstly, the filament temperature was slowly raised to about 1000°C and then to find and focus the Pb isotope signal. For NBS981 standard sample, ^{208}Pb signal was generally monitored, while for zircon sample, ^{206}Pb signal was generally monitored. Data acquisition was started when the ion beam reached the intensity as expected. During the SEM peak jump determination, the integration time was 8 s for ^{204}Pb and 4 s for the other Pb isotopes (^{205}Pb, ^{206}Pb, ^{207}Pb and ^{208}Pb). The settling time between peak jumps (idle time) was 1 s. Data were collected in 20 blocks with 25 cycles per block. The baseline measurement (with a integration time of 30 s), ion beam focusing and a peak-center program were performed every 5 blocks. Between each data block, the filament current was gently increased to maintain the signal intensity.

(2) U isotope determination. After the Pb isotope measurement, the filament temperature was further raised to about 1250°C to find and focus UO_2^+ isotope signal. When the $^{238}UO_2^+$ (mass 270) signal reached the expected intensity, data acquisition for U isotopes was started. The baseline measurement (the measurement time was 30 s), peak-centering and ion beam focusing were performed once at the start of data acquisition. Each data block collects 20 cycles of data and generally collecting 10 data blocks. The integration times for $^{235}UO_2^+$ and $^{238}UO_2^+$ was both set to 4 s and the idle time between peak jumps was 1 s. The filament current was gently increased up between each data block in the determination process to improve the UO_2^+ isotope signal intensity. The filament temperature was finally raised to about 1350°C and the measurement time of each sample was about 30 min.

(3) Data processing. The U-Pb data was processed by an offline Excel spreadsheet. Firstly, the Tripoli software was used to process the Pb and U isotope data derived from the TRITON Plus mass spectrometer. The Pb isotopic data with high ^{206}Pb/^{204}Pb were selected by the Tripoli software for statistical processing to get the Pb isotopic results for a sample (at least 80 cycles of data). Pb isotope fractionation effect was corrected by an external method using NBS981 Pb as a reference standard (Pb fractionation coefficient: 0.16± 0.08%, 2σ); ^{17}O/^{16}O=0.00039 and ^{18}O/^{16}O=0.00205 were used to correct the interference of $^{235}U^{17}O^{18}O$ with $^{238}U^{16}O_2$ for UO_2 isotope determination results (Condon et al., 2015; von Quadt et al., 2016). U isotope fractionation effect was corrected by an external method using U500 as a reference standard (U fractionation coefficient: 0.058±0.028%, 2σ). Final U-Pb date was calculated using the zircon U-Pb Excel calculation spreadsheet. The calculation included spike-subtraction, blank-correction, and then the calculations of Pb and U content, Pb isotope ratio, ^{206}Pb/^{238}U, ^{207}Pb/^{235}U, U-Pb ages and their errors. Among them, the analytical errors on the final U-Pb date took into account the effects of the main sources of error, such as instrument isotope ratio measurement error, fractionation correction error and blank-correction error. The final errors on the reported U-Pb ages further includes the tracer calibration error and the decay constant error, expressed in the form of ±X/Y/Z, where X is the internal (analytical) uncertainty, Y incorporates the U-Pb tracer calibration error, and Z includes the latter as well as the decay constant errors of Jaffey et al. (1971). Tracer calibration uncertainty (Y) must be taken into account when comparing

U-Pb dates from different techniques (e.g., ID-TIMS versus SIMS) or those produced using different tracers. When comparing dates for different decay systems (e.g., U-Pb versus Ar-Ar), the decay constant errors should be taken into account.

4.2 Analysis of organic carbon isotope composition of chert

Organic carbon isotope composition ($\delta^{13}C_{org}$) analysis was conducted at the laboratory for Stable Isotope Geochemistry, Institute of Geology and Geophysics.

Firstly, 2 g of chert powder sample crushed to 200 mesh was weighed and soaked overnight with 1 mol L^{-1} hydrochloric acid (HCl) until no bubbles were generated. Then, the acid solution was pipetted out, and the residue was washed with Milli-Q water repeatedly. After this step, the sample was dried in an oven at a temperature of 40°C overnight. 10–20 mg of the dried sample was weighed into a tin cup and then the wrapped sample was placed in the automatic sampler. The $\delta^{13}C$ values of samples were measured online by an elemental analyzer-gas isotope mass spectrometer (EA-IRMS) system (elemental analyzer model: Flash2000HT, mass spectrometer model: Delta V Advantage, Thermo Fisher Products) (Feng and Zhang, 2016). The measurement results are calculated against an international standard V-PDB and the analysis accuracy is better than 0.2‰.

5. Results

5.1 Zircon U-Pb ages

The zircons from the two K-bentonites in the top of the Liuchapo Formation are mostly 100 to 300 μm in length, 50 to 100 μm in width, with aspect ratios ranging from 2:1 to 6:1, indicative of typical volcanic origins (Figure 3).

CA-ID-TIMS U-Pb dating shows that the $^{206}Pb/^{238}U$ age ranges of zircons in the upper and lower K-bentonites are 535.81–537.46 Ma and 540.20–542.00 Ma, respectively (Table 1). The weighted mean $^{206}Pb/^{238}U$ age of the zircons in the upper and lower K-bentonites are 536.40±0.47/1.1/1.2 Ma (2σ, n=7, MSWD=0.92) and 541.48±0.46/1.1/1.2 Ma (2σ, n=8, MSWD=1.3) (Figure 4), respectively. We interpret the weighted mean $^{206}Pb/^{238}U$ ages as the crystallization ages of the volcanic zircons in the two K-bentonites, representing the sedimentary ages of the two K-bentonites.

5.2 Variations of $\delta^{13}C_{org}$ value

The $\delta^{13}C_{org}$ value of chert in the top of the Liuchapo Formation at the Pingyin section ranges from –36.71‰ to –27.95‰, with an overall variation of 9‰ and an average of –33.40‰. A significant positive and a subsequent significant

Table 1 Zircon CA-ID-TIMS U-Pb isotopic analyses of the two K-bentonites in the top of the Liuchapo Formation at the Pingyin section, South China[a)]

Analysis point	Pb_c (pg)	Pb^*/Pb_c	Th/U	$^{206}Pb/^{204}Pb$	$^{208}Pb/^{206}Pb$
PY-LB-1	3.5	5.2	0.33	335	0.2091
PY-LB-2	2.8	7.7	0.35	488	0.1821
PY-LB-3	3.1	6.0	0.87	342	0.3664
PY-LB-4	3.7	7.7	0.34	490	0.1784
PY-LB-5	5.2	2.2	0.77	140	0.4780
PY-LB-6	3.6	2.9	0.53	188	0.3489
PY-LB-7	2.9	5.0	0.47	314	0.2589
PY-13-1	2.1	15.9	1.15	821	0.3972
PY-13-2	5.6	5.0	0.67	298	0.3211
PY-13-3	2.2	10.9	0.30	695	0.1447
PY-13-4	4.0	12.0	1.30	602	0.4568
PY-13-5	2.1	11.6	0.33	730	0.1531
PY-13-6	5.2	9.5	0.60	560	0.2491
PY-13-7	3.7	25.6	0.44	15496	0.1585
PY-13-8	3.1	7.4	0.45	456	0.2164

Analysis point	Isotope ratio					
	$^{206}Pb/^{238}U$	2σ (%)	$^{207}Pb/^{235}U$	2σ (%)	$^{207}Pb/^{206}Pb$	2σ (%)
PY-LB-1	0.08667	0.24	0.7033	2.1	0.05888	0.36
PY-LB-2	0.08669	0.21	0.7003	1.4	0.05861	0.34
PY-LB-3	0.08675	0.22	0.7070	2.1	0.05913	0.59
PY-LB-4	0.08675	0.21	0.6987	1.4	0.05844	0.30
PY-LB-5	0.08687	0.47	0.7182	5.1	0.05999	0.87
PY-LB-6	0.08689	0.37	0.7110	3.9	0.05937	0.81
PY-LB-7	0.08695	0.24	0.7045	2.3	0.05879	0.45
PY-13-1	0.08741	0.19	0.70441	0.89	0.05847	0.25
PY-13-2	0.08758	0.27	0.7186	2.3	0.05953	0.41
PY-13-3	0.08762	0.18	0.7124	1.1	0.05899	0.36
PY-13-4	0.08763	0.17	0.7005	1.2	0.05800	0.25
PY-13-5	0.08763	0.17	0.7033	1.0	0.05824	0.27
PY-13-6	0.08767	0.19	0.7100	1.2	0.05876	0.28
PY-13-7	0.08769	0.15	0.70699	0.48	0.05850	0.13
PY-13-8	0.08771	0.20	0.7024	1.5	0.05810	0.33

Analysis point	Age					
	$^{206}Pb/^{238}U$ (Ma)	2σ (%)	$^{207}Pb/^{235}U$ (Ma)	2σ (%)	$^{207}Pb/^{206}Pb$ (Ma)	Relative error
PY-LB-1	535.81	0.23	540.8	1.6	563	0.03
PY-LB-2	535.93	0.20	539.0	1.1	553	0.04
PY-LB-3	536.27	0.21	542.9	1.6	572	0.02
PY-LB-4	536.29	0.20	538.0	1.1	546	0.06
PY-LB-5	536.98	0.45	549.6	4.0	603	0.01
PY-LB-6	537.14	0.36	545.4	3.0	581	0.02
PY-LB-7	537.46	0.23	541.5	1.8	559	0.02
PY-13-1	540.20	0.18	541.42	0.69	548	0.11
PY-13-2	541.21	0.25	549.8	1.8	587	0.04
PY-13-3	541.45	0.17	546.14	0.81	567	0.06
PY-13-4	541.50	0.16	539.10	0.90	530	0.06
PY-13-5	541.52	0.16	540.78	0.78	539	0.08
PY-13-6	541.75	0.18	544.74	0.94	558	0.07
PY-13-7	541.86	0.15	542.96	0.37	549	0.13
PY-13-8	542.00	0.19	540.2	1.2	534	0.03

a) (1) Pb_c stands for common lead, which was assumed to be from laboratory blank; Pb^* stands for radiogenic lead; (2) the blank subtraction calculation was based on the long-term laboratory Pb blank isotope ratio measurement results: $^{206}Pb/^{204}Pb$=17.78±0.50 (2σ), $^{207}Pb/^{204}Pb$=15.31±0.34 (2σ); (3) the ^{205}Pb-^{235}U spike was calibrated against standard solutions prepared from NIST981 Pb and GBW04205 U_3O_8. The calibration error on U/Pb ratio of ^{205}Pb-^{235}U is ~0.18% (2RSE).

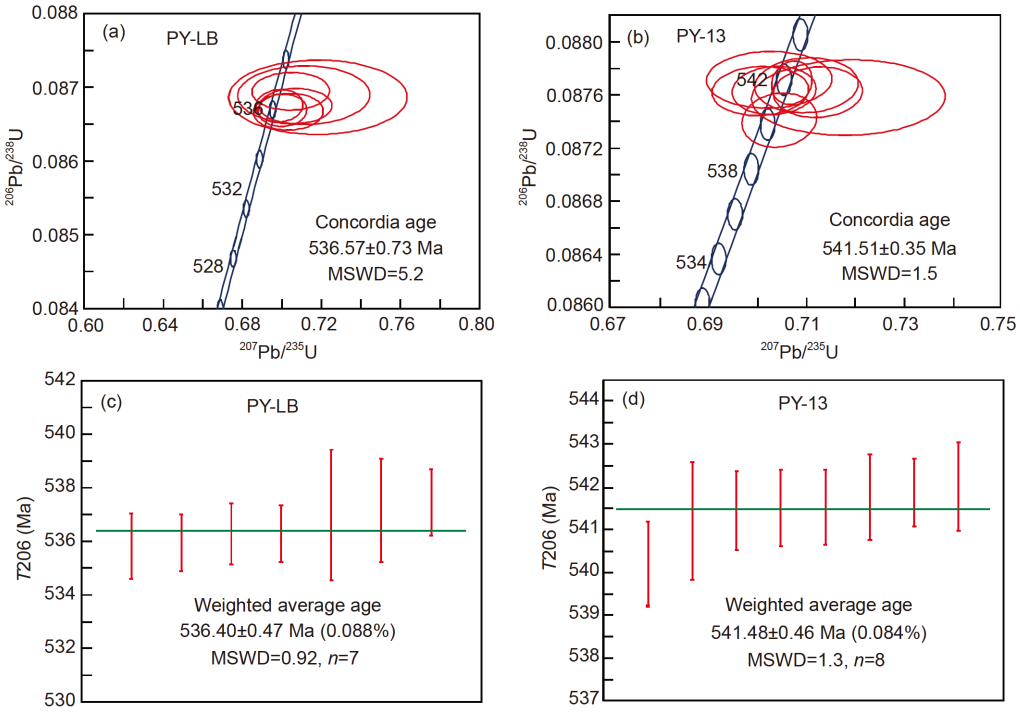

Figure 4 U-Pb dates of zircons in the two K-bentonites in the top of the Liuchapo Formation at the Pingyin section, South China. Ellipse and error line of data points represent 2σ uncertainty, *T*206 represents $^{206}Pb/^{238}U$ age.

negative excursion were recorded in this interval. Specifically, the $\delta^{13}C_{org}$ value has a rising trend at 4.65–2.74 m below the upper boundary of the Liuchapo Formation, representing an obvious positive excursion. A decreasing trend and a significant negative excursion occur at 2.25–2.09 m beneath the boundary. The $\delta^{13}C_{org}$ value of the cherts at 2.09–0.6 m below the boundary tends to be stable, with an average of –34.94‰. There is a small $\delta^{13}C_{org}$ fluctuation at 0.5 m under the boundary (Table 2; Figure 5).

6. Discussion

6.1 Improvement of the temporal framework of the Liuchapo Formation

Previous works have already constructed an initial temporal framework for the Liuchapo Formation in the deep-water realm in South China. Zhou et al. (2018) reported a preliminary SHRIMP U-Pb age of 550±3 Ma for zircons from a K-bentonite at the bottom of the Liuchapo Formation at the Fanglong section, Guizhou Province. Yang et al. (2017) provided a precise CA-ID-TIMS U-Pb age of 545.76±0.66 Ma for zircons in a K-bentonite in the lower part of the Liuchapo Formation at the Longbizui section, Hunan Province. Zhou et al. (2013) conducted a SHRIMP U-Pb dating on zircons in the K-bentonite (the older one in this study) in the top of the Liuchapo Formation at the Pingyin section. The weighted mean U-Pb age of 12 zircons they obtained is 536 ±5 Ma, thus obtaining preliminary age information for the topmost interval of the Liuchapo Formation. Chen D et al. (2015) carried out a SIMS U-Pb geochronology study on zircons of an ash bed from the top of the Liuchapo Formation at the Bahuang section, which is near the Pingyin section. The weighted mean age of 18 zircons in the ash is 542.6±3.7

Table 2 Organic carbon isotopic composition of cherts in the topmost Liuchapo Formation at the Pingyin section, South China

Sample	$\delta^{13}C_{org}$ (‰)	Sample	$\delta^{13}C_{org}$ (‰)	Sample	$\delta^{13}C_{org}$ (‰)	Sample	$\delta^{13}C_{org}$ (‰)
LB-1	–35.12	LB-8	–29.97	LB-15	–32.69	LB-22	–34.68
LB-2	–34.62	LB-9	–30.62	LB-16	–29.57	LB-23	–34.95
LB-3	–35.48	LB-10	–31.10	LB-17	–31.27	LB-24	–34.78
LB-4	–34.81	LB-11	–29.82	LB-18	–35.36	LB-25	–33.88
LB-5	–34.42	LB-12	–27.95	LB-19	–35.11	LB-26	–36.71
LB-6	–29.58	LB-13	–31.85	LB-20	–35.34	LB-27	–34.78
LB-7	–34.02	LB-14	–32.36	LB-21	–35.32	LB-28	–34.65

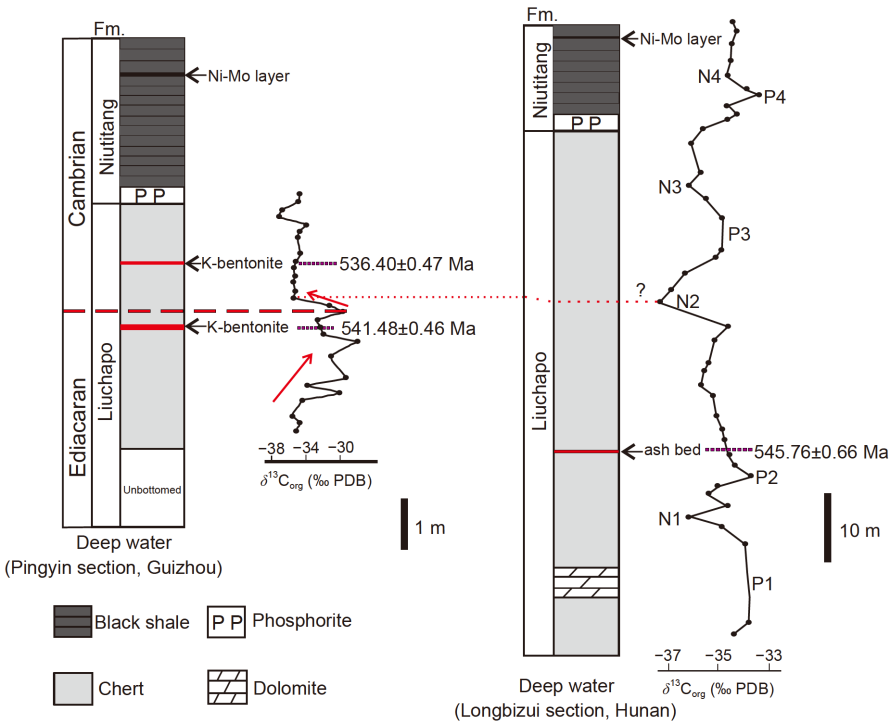

Figure 5 Secular change in organic carbon isotope composition of the Liuchapo Formation at the Pingyin and Longbizui sections in South China. The organic carbon isotope data of the Longbizui section are derived from Wang et al. (2012), and the high-precision age of this section is from Yang et al. (2017).

Ma. This result is consistent with that reported by Zhou et al. (2013) within uncertainties, which further verifies the sedimentary age information of the topmost Liuchapo Formation. However, the SHRIMP/SIMS U-Pb dating technique can only achieve an accuracy at 1% (Ireland and Williams, 2003; Yang et al., 2014). Thus, the precision of the two U-Pb ages from the topmost Liuchapo Formation is still very low, which limits their application in regional and international stratigraphic correlation.

In this study, further zircon CA-ID-TIMS U-Pb dating for the same K-bentonite (PY-13) studied by Zhou et al. (2013) was carried out and the result was 541.48±0.46/1.1/1.2 Ma. This age is basically consistent with the previous SHRIMP U-Pb age within analytical error. However, the precision of the age has been significantly improved and thus the age can be used for stratigraphic correlation. At the same time, we obtained the zircon CA-ID-TIMS U-Pb age of 536.40±0.47/1.1/1.2 Ma for the newly discovered K-bentonite (PY-LB) at the Pingyin section. The high-precision zircon CA-ID-TIMS U-Pb age data in this study undoubtedly improved the temporal framework of the Liuchapo Formation (Figure 5).

The above new and more detailed temporal framework for the Liuchapo Formation indicates that the topmost interval of the formation is extremely condensed, which can be reflected by the Pingyin and Bahuang sections. The thickness of the strata between the two K-bentonites in the top of the Liuchapo Formation at the Pingyin section is 1.2 m. According to the age data of the K-bentonites, the average accumulation rate for this interval ranges from 0.21 to 0.27 mm ka^{-1}. The ages of the two tuffaceous beds at the Liuchapo-Niutitang boundary and 4.15 m below the boundary are 522.3±3.7 Ma and 542.6±3.7 Ma, respectively (Chen D et al., 2015), which constrain an average deposition rate range of 0.16–0.28 mm ka^{-1} for the strata between the two tuffaceous beds. Some workers have reported examples with extremely low accumulation rate in history and modern oceans. In anoxic sedimentary environments of the modern and Holocene Black Sea, the deposition rate of organic carbon-rich sediments can be as low as 1 mm ka^{-1} (Stein, 1990). The polymetallic enrichment in the basal Niutitang Formation in South China has been considered as a result of extremely low accumulation rate (about 1 mm ka^{-1}) in the ocean (Mao et al., 2002; Lehmann et al., 2007). Although the cause of such a low deposition rate for the topmost Liuchapo Formation needs further interpretation, its tectonic background of sea level rise (Chen D et al., 2015) may be one of the reasons. The occurrence of organic carbon-rich black shale laminae, the increase of organic carbon content in cherts, and the gradual enrichment of multiple metal elements (unpublished data) of this interval may be the response to the sedimentary environment with extremely low deposition rate.

6.2 Constraints on the Ediacaran-Cambrian boundary in deep-water realm in South China

The Global Stratotype Section and Point (GSSP) for the

Ediacaran-Cambrian boundary, defining the first appearance data (FAD) of the trace fossil *Treptichnus pedum* at Fortune Head in Newfoundland, Canada, has been ratified by the International Union of Geological Science (IUGS) in 1992. The specific horizon is 2.4 m above the lower boundary of Member 2 of the Chapel Island Formation at the section (Brasier et al., 1994; Landing, 1994). However, since the GSSP has been ratified, scholars have gradually found its defects. Recently, Zhu et al. (2019) have analyzed the detailed shortcomings and global correlation dilemma of the GSSP. The main defects they pointed out are: (1) Due to the discovery of trace fossil *T. pedum* (Gehling et al., 2001) at 4.41 m below the GSSP of the Ediacaran-Cambrian boundary, some workers have attempted to revise the definition of the boundary (Landing et al., 2013; Geyer and Landing, 2016; Buatois, 2018). However, the new definition is vague and there is no specific point can be used for the boundary. (2) Increasing biostratigraphic research found that *T. pedum* coexists with typical Ediacaran organisms in some areas (Jensen et al., 2000; Jensen and Runnegar, 2005; Macdonald et al., 2014), or that the FAD of *T. pedum* in some regions is above the horizon rich in small shelly fossils (Zhu, 1997; Rogov et al., 2015). (3) As the lithology at Fortune Head is mainly silisiclastic, it lacks volcanic material layer that can obtain radiometric age, and it also lacks lithology that can obtain carbon isotope composition record. Thus it limits the global correlation of the boundary.

So far, geologists have adopted various criteria for the Ediacaran-Cambrian boundary in different regions (Qian et al., 1996; Zhu, 1997; Zhang and Zhu, 1979; Qian et al., 2002; Zhu et al., 2001, 2003; Amthor et al., 2003; Bowring et al., 2007; Khomentovsky and Karlova, 2005; Rozanov et al., 2010; Zhamoida, 2015). In view of this situation, it is urgent to find other widely correlatable standards for the Ediacaran-Cambrian boundary. Zhu et al. (2019) listed several potential indicators for the Ediacaran-Cambrian boundary: (1) the FAD of *T. pedum*; (2) the FAD of typical Cambrian small shelly fossils *Anabarites trisulcatus* and *Protohertzina anabarica*; (3) the FAD of the *Asteridium-Heliosphaeridium-Comasphaeridium* (AHC) acritarch assemblage; (4) the BAsal Cambrian Carbon Isotope Excursion (BACE, Zhu et al., 2006), and high-precision radiometric ages of the corresponding horizons. At present, there is a certain degree of uncertainty in each of the above-mentioned potential indicators and the sequential relationship between them is not very clear (Zhu et al., 2019). Zhu et al. (2019) emphasized that the BACE should be used as a preferred reference standard for the Ediacaran-Cambrian boundary, when the above biostratigraphic standards cannot reach a consensus. At the same time, they suggest that the boundary should be placed at the bottom of the BACE, specifically at the onset of decreasing $\delta^{13}C$ values from the terminal Ediacaran positive carbon isotope plateau (EPIP) to the BACE. The proposal of Zhu et al. (2019) has obvious feasibility in practice, because the BACE has been recognized in the Ediacaran-Cambrian transitional strata in various regions of the world (Magaritz et al., 1986, 1991; Zhang et al., 1997; Kimura et al., 1997; Zhu et al., 2006, 2017a; Kouchinsky et al., 2007; Li et al., 2009, 2013; Maloof et al., 2010; Smith et al., 2016a, 2016b). Therefore, this chemostratigraphic marker can be used to find and determine the Ediacaran-Cambrian boundary, especially in strata lacking fossils.

Up to now, a series of advances have been made in radiometric age constraint on the Ediacaran-Cambrian boundary. Currently, the age (541 Ma) used for the boundary in the international chronostratigraphic chart is from an ash bed in Member A_4C of the Ara Group in Oman. The first reported zircon U-Pb CA-TIMS age of the ash is 542±0.3 Ma (Amthor et al., 2003). Since then, the age data have been revised to 541.00±0.13 Ma (Bowring et al., 2007) and 541.00 ±0.29 Ma (Schmitz, 2012). The ash is located at the bottom of the BACE, but its sequence relationship to *T. pedum* remains unclear. In addition, the BACE recorded in the Ara Group is incomplete, which does not rule out the possibility of sedimentary discontinuity (Zhu et al., 2019). Therefore, constraining the Ediacaran-Cambrian boundary by the age of the ash, is not the best choice. An ash bed in the upper Spitskopf Member of the topmost Nama Group in southern Namibia can also provide the reference age of the Ediacaran-Cambrian boundary. The first reported zircon U-Pb CA-TIMS age of the ash is 543.3±1 Ma (Grotzinger et al., 1995), which was recently revised to 540.61±0.67 Ma (Schmitz, 2012). This ash coexists with typical Ediacaran soft body fossils (Grotzinger et al., 1995) and is located within the EPIP. It is obviously lower than the BACE (Wood et al., 2015) and thus its age (540.61±0.67 Ma) should be the maximum age of the current Ediacaran-Cambrian boundary (Zhu et al., 2019). Recently, Linnemann et al. (2019) carried out zircon U-Pb CA-ID-TIMS dating on newly discovered ash beds in the upper Spitskopf Member of the topmost Nama Group. They considered the age of the Ediacaran-Cambrian boundary suggested by them to be 538.6–538.8 Ma. Preliminary U-Pb ages of 540.7–539.6 Ma for volcanic zircons from the basal BACE in several sections in Yunnan Province, China (Zhu et al., 2015, 2017b), also indicates the age of the Ediacaran-Cambrian boundary should be close to and less than 539.6 Ma (Zhu et al., 2019).

The Ediacaran-Cambrian transitional strata (Liuchapo Formation or its equivalents) in the deep-water realm of the Yangtze Platform in South China are mainly composed of cherts rich in organic carbon. Fossils in the strata are scarce. However, several negative organic carbon isotope anomalies have been recorded in them. Previous studies revealed coupling of organic and inorganic carbon isotopes during the Ediacaran-Cambrian transition period (Kaufman and Knoll, 1995; Shen and Schidlowski, 2000; Ishikawa et al., 2008;

Chen D et al., 2015). Therefore, the Ediacaran-Cambrian boundary in the deep-water area in South China could be determined by one of the negative organic carbon isotope excursions. Several sections of the Liuchapo Formation (or its equivalents) in South China documented similar organic carbon isotope trend (Goldberg et al., 2007; Guo et al., 2007, 2013; Chen et al., 2009; Wang et al., 2012; Wang et al., 2014). Among them, the organic carbon isotope curve from the Longbizui section in Hunan Province is the most complete. Three positive (P1–P3) and three negative (N1–N3) organic carbon isotope excursions (Figure 5) were recorded in the section (Wang et al., 2012). Some workers (Wang et al., 2012; Yang et al., 2017; Chen D et al., 2015) thought that the second negative excursion (N2) is equivalent to the BACE and regarded the excursion N2 as the Ediacaran-Cambrian boundary in the deep-water realm in South China. This scheme is supported by the preliminary SIMS U-Pb age data (Chen D et al., 2015). However, it still needs high-precision zircon CA-ID-TIMS U-Pb ages to confirm. In this study, a significant negative organic carbon isotope excursion has been identified between the two K-bentonites in the topmost Liuchapo Formation at the Pingyin section. Zircon U-Pb CA-ID-TIMS ages of the two K-bentonites constrains it between 541.48±0.46/1.1/1.2 Ma and 536.40±0.47/1.1/1.2 Ma. Based on the above-mentioned potential indicators and the geochronological advances for the Ediacaran-Cambrian boundary, we believe that the boundary in the Pingyin section should be placed at the horizon doucumented the excursion. The horizon recorded the excursion in the Pingyin section is a critical one which is first well constrained by the high-precision zircon U-Pb CA-ID-TIMS ages in deep-water realm in South China. It is valuable for unravelling the information of the paleo-ocean during the Ediacaran-Cambrian period.

6.3 Significance to paleo-ocean environment

In this study, the Ediacaran-Cambrian boundary, which we determined in the Pingyin section, is of great significance to the research of the global paleo-ocean environment during the Ediacaran-Cambrian transitional period. From the terminal Ediacaran to the earliest Cambrian, the life evolution has undergone significant changes, which is manifested in a gradual and multi-stage biological radiation process accompanying the extinction of Ediacaran organisms. As for the cause of the extinction of organisms, scholars have put forward various hypotheses, such as extraterrestrial impact, volcanic eruption, ocean anoxia, etc. Wille et al. (2008) conducted a Mo isotope research on the Ni-Mo layer and its overlying black shales in the basal Niutitang Formation in South China, together with the black shales overlying the Ediacaran-Cambrian boundary in Oman. They believed a global anoxic event which resulted from the upwelling of deep hydrogen sulfide-rich seawater and the release of hydrogen sulfide into the surface water, caused the extinction of Ediacaran organisms. However, some workers (Jiang et al., 2009; Lan et al., 2017) questioned the globality of the anoxic event. The reason is that the zircon SHRIMP U-Pb age (532.3±0.7 Ma) of an ash bed at the basal Niutitang Formation at the Songlin section is obviously younger than the age of the Ediacaran-Cambrian boundary. Therefore, considering the Ni-Mo layer as the Ediacaran-Cambrian boundary and correlating it with the Ediacaran-Cambrian boundary in Oman, to support the globality of the anoxic event is debatable. Wille et al. (2009) argued that the zircon U-Pb age provided by Jiang et al. (2009) were obtained by SHRIMP method, which is supposed to be significantly younger than the age obtained by CA-ID-TIMS method. Therefore, Wille et al. (2009) still adhered to their original views (Wille et al., 2008). Meanwhile, they proposed a prospect that further zircon CA-ID-TIMS U-Pb geochronological works are needed to clarify this issue (Wille et al., 2009). In this study, we carried out zircon CA-ID-TIMS U-Pb dating on the newly discovered K-bentonites. The results constrain the Ediacaran-Cambrian boundary in the deep-water area in South China at the top of the Liuchapo Formation, rather than at the Ni-Mo layer in the basal Niutitang Formation. In combination with the noticeable vertical distance between the Ediacaran-Cambrian boundary and Ni-Mo layer (Figure 5) and the extremely condensed feature of this interval, the results suggest that the anoxic event recorded in the Ni-Mo layer and its overlying strata in South China should be different from that near the Ediacaran-Cambrian boundary in Oman. Therefore, the globality of the anoxic event near the Ediacaran-Cambrian boundary proposed by Wille et al. (2008) still needs new robust evidences.

The results of high-precision zircon CA-ID-TIMS U-Pb geochronology in this study suggest that the further research of the paleo-ocean environment near the Ediacaran-Cambrain boundary in south China should focus on the topmost Liuchapo Formation and its equivalents, to determine whether there is evidence supporting the global anoxic hypothesis near the Ediacaran-Cambrian boundary proposed by Wille et al. (2008). Chen X et al. (2015) carried out Mo isotope analysis on the top of the Liuchapo Formation and its equivalent strata in deep-water area in South China. The results show that the variation trend of Mo isotope recorded in this interval is consistent with that recorded near the the Ediacaran-Cambrian boundary in Oman reported by Wille et al. (2008). Therefore, although the correlation of the Ediacaran-Cambrian boundary between Oman and China by Wille et al. (2008) is controvential, the hypothesis of Wille et al. (2008) could be directly supported by Mo isotope evidence from the top of the Liuchapo Formation and its equivalents (Chen X et al., 2015), if our proposal for the Ediacaran-Cambrian boundary in South China was invoked.

The reconciliation by the newly Ediacaran-Cambrian boundary scheme on the controversy of the globality of the anoxic event near the Ediacaran-Cambrian boundary, agrees well with the viewpoint that an anoxic event exists near the Ediacaran-Cambrian boundary in South China (Wei et al., 2018; Wang et al., 2018; Li et al., 2019), based on other geochemical evidences (e.g. $\delta^{238}U$, $\delta^{15}N$, $\delta^{34}S_{py}$ and $\Delta^{33}S_{py}$, etc.).

7. Conclusions

Through a CA-ID-TIMS U-Pb dating on zircons from two K-bentonites in the topmost Liuchapo Formation at the Pingyin section on the Yangtze Platform in South China, and an organic carbon isotope analysis of the cherts in the same interval, the following conclusions were obtained:

(1) The sedimentary ages of the two K-bentonites are 536.40±0.47/1.1/1.2 Ma (2σ, n=7, MSWD=0.92) and 541.48 ±0.46/1.1/1.2 Ma (2σ, n=8, MSWD=1.3), respectively.

(2) The Ediacaran-Cambrian boundary at the Pingyin section is constrained at the horizon between the two K-bentonites in the topmost Liuchapo Formation, which documented a significant negative organic carbon isotope excursion.

(3) The determination of the Ediacaran-Cambrian boundary suggests that the hypothesis of a global anoxic event near the Ediacaran-Cambrian boundary could be supported by evidences from the top of the Liuchapo Formation or its equivalents in South China.

Acknowledgements *We thank Lianjun Feng, Zhongwu Lan and Xiqiang Zhou for their helpful suggestions on this work. We are grateful to the two reviewers and the executive Editor-in-Chief for their constructive comments that have significantly improved the quality of this paper. We thank Hongwei Li for his technical support in the organic carbon isotope experiment. We are grateful to Hua Yang and Di Zhang from Guizhou Normal University for their assistance in sample collection. This work was supported by the National Natural Science Foundation of China (Grant Nos. 41673061, 41462001 & 41688103) and the Chinese Academy of Sciences Instrument and Equipment Function Development Project (Grant No. IGG201803).*

References

Amthor J E, Grotzinger J P, Schröder S, Bowring S A, Ramezani J, Martin M W, Matter A. 2003. Extinction of *Cloudina* and *Namacalathus* at the Precambrian-Cambrian boundary in Oman. Geology, 31: 431–434

Bowring S A, Grotzinger J P, Condon D J, Ramezani J, Newall M J, Allen P A. 2007. Geochronologic constraints on the chronostratigraphic framework of the Neoproterozoic Huqf Supergroup, Sultanate of Oman. Am J Sci, 307: 1097–1145

Brasier M D, Corfield R M, Derry L A, Rozanov A Y, Zhuravlev A Y. 1994. Multiple $\delta^{13}C$ excursions spanning the Cambrian explosion to the Botomian crisis in Siberia. Geology, 22: 455–458

Buatois L A. 2018. *Treptichnus pedum* and the Ediacaran-Cambrian boundary: Significance and caveats. Geol Mag, 155: 174–180

Canfield D E, Poulton S W, Knoll A H, Narbonne G M, Ross G, Goldberg T, Strauss H. 2008. Ferruginous conditions dominated later Neoproterozoic deep-water chemistry. Science, 321: 949–952

Cawood P A, Wang Y, Xu Y, Zhao G. 2013. Locating South China in Rodinia and Gondwana: A fragment of greater India lithosphere? Geology, 41: 903–906

Chen D, Wang J, Qing H, Yan D, Li R. 2009. Hydrothermal venting activities in the Early Cambrian, South China: Petrological, geochronological and stable isotopic constraints. Chem Geol, 258: 168–181

Chen D, Zhou X, Fu Y, Wang J, Yan D. 2015. New U-Pb zircon ages of the Ediacaran-Cambrian boundary strata in South China. Terra Nova, 27: 62–68

Chen X, Ling H F, Vance D, Shields-Zhou G A, Zhu M, Poulton S W, Och L M, Jiang S Y, Li D, Cremonese L, Archer C. 2015. Rise to modern levels of ocean oxygenation coincided with the Cambrian radiation of animals. Nat Commun, 6: 7142

Chu Z Y, Xu J J, Chen Z, Li C F, He H Y, Li X H, Guo J H. 2016. Ultra-low blank analytical procedure for high precision CA-ID-TIMS U-Pb dating of single grain zircons (in Chinese). Chin Sci Bull, 61: 1121–1129

Condon D J, Schoene B, McLean N M, Bowring S A, Parrish R R. 2015. Metrology and traceability of U-Pb isotope dilution geochronology (EARTHTIME Tracer Calibration Part I). Geochim Cosmochim Acta, 164: 464–480

Erwin D H, Laflamme M, Tweedt S M, Sperling E A, Pisani D, Peterson K J. 2011. The Cambrian conundrum: Early divergence and later ecological success in the early history of animals. Science, 334: 1091–1097

Feng L, Zhang Q. 2016. The Pre-Sturtian negative $\delta^{13}C$ excursion of the Dajiangbian formation deposited on the western margin of Cathaysia Block in south China. J Earth Sci, 27: 225–232

Gehling J G, Jensen S, Droser M L, Myrow P M, Narbonne G M. 2001. Burrowing below the basal Cambrian GSSP, fortune head, Newfoundland. Geol Mag, 138: 213–218

Gerstenberger H, Haase G. 1997. A highly effective emitter substance for mass spectrometric Pb isotope ratio determinations. Chem Geol, 136: 309–312

Geyer G, Landing E. 2016. The Precambrian-Phanerozoic and Ediacaran-Cambrian boundaries: A historical approach to a dilemma. Geol Soc Lond Spec Publ, 448: 311–349

Goldberg T, Strauss H, Guo Q, Liu C. 2007. Reconstructing marine redox conditions for the Early Cambrian Yangtze Platform: Evidence from biogenic sulphur and organic carbon isotopes. Palaeogeogr Palaeoclimatol Palaeoecol, 254: 175–193

Grotzinger J P, Bowring S A, Saylor B Z, Kaufman A J. 1995. Biostratigraphic and geochronologic constraints on early animal evolution. Science, 270: 598–604

Guo Q J, Strauss H, Zhu M Y, Zhang J M, Yang X L, Lu M, Zhao F C. 2013. High resolution organic carbon isotope stratigraphy from a slope to basinal setting on the Yangtze Platform, South China: Implications for the Ediacaran-Cambrian transition. Precambrian Res, 225: 209–217

Guo Q J, Strauss H, Liu C Q, Goldberg T, Zhu M, Pi D, Heubeck C, Vernhet E, Yang X, Fu P. 2007. Carbon isotopic evolution of the terminal Neoproterozoic and early Cambrian: Evidence from the Yangtze Platform, South China. Palaeogeogr Palaeoclimatol Palaeoecol, 254: 140–157

Ireland T R, Williams I S. 2003. Considerations in zircon geochronology by SIMS. Rev Mineral Geochem, 53: 215–241

Ishikawa T, Ueno Y, Komiya T, Sawaki Y, Han J, Shu D, Li Y, Maruyama S, Yoshida N. 2008. Carbon isotope chemostratigraphy of a Precambrian/Cambrian boundary section in the Three Gorge area, South China: Prominent global-scale isotope excursions just before the Cambrian explosion. Gondwana Res, 14: 193–208

Jaffey A H, Flynn K F, Glendenin L E, Bentley W C, Essling A M. 1971. Precision measurement of half-lives and specific activities of ^{235}U and ^{238}U. Phys Rev C, 4: 1889–1906

Jensen S, Runnegar B N. 2005. A complex trace fossil from the Spitskop Member (terminal Ediacaran-Lower Cambrian) of southern Namibia. Geol Mag, 142: 561–569

Jensen S, Saylor B Z, Gehling J G, Germs G J B. 2000. Complex trace fossils from the terminal Proterozoic of Namibia. Geology, 28: 143–146
Jiang S Y, Pi D H, Heubeck C, Frimmel H, Liu Y P, Deng H L, Ling H F, Yang J H. 2009. Early Cambrian ocean anoxia in South China. Nature, 459: E5–E6
Jiang S Y, Yang J H, Ling H F, Chen Y Q, Feng H Z, Zhao K D, Ni P. 2007. Extreme enrichment of polymetallic Ni-Mo-PGE-Au in Lower Cambrian black shales of South China: An Os isotope and PGE geochemical investigation. Palaeogeogr Palaeoclimatol Palaeoecol, 254: 217–228
Kaufman A, Knoll A. 1995. Neoproterozoic variations in the C-isotopic composition of seawater: Stratigraphic and biogeochemical implications. Precambrian Res, 73: 27–49
Khomentovsky V V, Karlova G A. 2005. The Tommotian Stage base as the Cambrian Lower Boundary in Siberia. Stratigr Geol Correl, 13: 21–34
Kimura H, Matsumoto R, Kakuwa Y, Hamdi B, Zibaseresht H. 1997. The Vendian-Cambrian δ^{13}C record, North Iran: Evidence for overturning of the ocean before the Cambrian Explosion. Earth Planet Sci Lett, 147: E1–E7
Kouchinsky A, Bengtson S, Pavlov V, Runnegar B, Torssander P, Young E, Ziegler K. 2007. Carbon isotope stratigraphy of the Precambrian-Cambrian Sukharikha River section, northwestern Siberian platform. Geol Mag, 144: 609–618
Lan Z, Li X H, Chu X, Tang G, Yang S, Yang H, Liu H, Jiang T, Wang T. 2017. SIMS U-Pb zircon ages and Ni-Mo-PGE geochemistry of the lower Cambrian Niutitang Formation in South China: Constraints on Ni-Mo-PGE mineralization and stratigraphic correlations. J Asian Earth Sci, 137: 141–162
Landing E. 1994. Precambrian-Cambrian boundary global stratotype ratified and a new perspective of Cambrian time. Geology, 22: 179–182
Landing E, Geyer G, Brasier M D, Bowring S A. 2013. Cambrian Evolutionary Radiation: Context, correlation, and chronostratigraphy—Overcoming deficiencies of the first appearance datum (FAD) concept. Earth-Sci Rev, 123: 133–172
Lehmann B, Nägler T F, Holland H D, Wille M, Mao J, Pan J, Ma D, Dulski P. 2007. Highly metalliferous carbonaceous shale and Early Cambrian seawater. Geology, 35: 403–406
Li D, Ling H F, Shields-Zhou G A, Chen X, Cremonese L, Och L, Thirlwall M, Manning C J. 2013. Carbon and strontium isotope evolution of seawater across the Ediacaran-Cambrian transition: Evidence from the Xiaotan section, NE Yunnan, South China. Precambrian Res, 225: 128–147
Li D, Ling H F, Jiang S Y, Pan J Y, Chen Y Q, Cai Y F, Feng H Z. 2009. New carbon isotope stratigraphy of the Ediacaran-Cambrian boundary interval from SW China: Implications for global correlation. Geol Mag, 146: 465–484
Li D, Zhang X, Hu D, Li D, Zhang G, Zhang X, Ling H F, Xu Y, Shen Y. 2019. Multiple S-isotopic constraints on paleo-redox and sulfate concentrations across the Ediacaran-Cambrian transition in South China. Precambrian Res, 105500
Li Z X, Bogdanova S V, Collins A S, Davidson A, De Waele B, Ernst R E, Fitzsimons I C W, Fuck R A, Gladkochub D P, Jacobs J, Karlstrom K E, Lu S, Natapov L M, Pease V, Pisarevsky S A, Thrane K, Vernikovsky V. 2008. Assembly, configuration, and break-up history of Rodinia: A synthesis. Precambrian Res, 160: 179–210
Linnemann U, Ovtcharova M, Schaltegger U, Gärtner A, Hautmann M, Geyer G, Vickers-Rich P, Rich T, Plessen B, Hofmann M, Zieger J, Krause R, Kriesfeld L, Smith J. 2019. New high-resolution age data from the Ediacaran-Cambrian boundary indicate rapid, ecologically driven onset of the Cambrian explosion. Terra Nova, 31: 49–58
Macdonald F A, Pruss S B, Strauss J V. 2014. Trace fossils with spreiten from the Late Ediacaran Nama Group, Namibia: Complex feeding patterns five million years before the Precambrian Cambrian boundary. J Paleontol, 88: 299–308
Magaritz M, Holser W T, Kirschvink J L. 1986. Carbon-isotope events across the Precambrian/Cambrian boundary on the Siberian Platform. Nature, 320: 258–259
Magaritz M, Kirschvink J L, Latham A J, Zhuravlev A Y, Rozanov A Y. 1991. Precambrian/Cambrian boundary problem: Carbon isotope correlations for Vendian and Tommotian time between Siberia and Morocco. Geology, 19: 847–850
Maloof A C, Porter S M, Moore J L, Dudas F O, Bowring S A, Higgins J A, Fike D A, Eddy M P. 2010. The earliest Cambrian record of animals and ocean geochemical change. Geol Soc Am Bull, 122: 1731–1774
Mao J, Lehmann B, Du A, Zhang G, Ma D, Wang Y, Zeng M, Kerrich R. 2002. Re-Os dating of polymetallic Ni-Mo-PGE-Au mineralization in lower Cambrian black shales of South China and its geologic significance. Econ Geol, 97: 1051–1061
Mattinson J M. 2005. Zircon U-Pb chemical abrasion ("CA-TIMS") method: Combined annealing and multi-step partial dissolution analysis for improved precision and accuracy of zircon ages. Chem Geol, 220: 47–66
Qian Y, Zhu M Y, He T G, Jiang Z W. 1996. New investigation of Precambrian- Cambrian boundary sections in eastern Yunnan (in Chinese with English abstract). Acta Micropal Sin, 13: 225–240
Qian Y, Zhu M Y, Li G X, Jiang Z W, Van Iten H. 2002. A supplemental Precambrian-Cambrian boundary global stratotype section in SW China. Acta Palaeontol Sin, 41: 19–26
von Quadt A, Wotzlaw J F, Buret Y, Large S J E, Peytcheva I, Trinquier A. 2016. High-precision zircon U/Pb geochronology by ID-TIMS using new 1013 ohm resistors. J Anal At Spectrom, 31: 658–665
Rogov V I, Karlova G A, Marusin V V, Kochnev B B, Nagovitsin K E, Grazhdankin D V. 2015. Duration of the first biozone in the Siberian hypostratotype of the Vendian. Rus Geol Geophys, 56: 573–583
Rozanov A Y, Khomentovsky V V, Shabanov Y Y, Karlova G A, Varlamov A I, Luchinina V A, Pegel' T V, Demidenko Y E, Parkhaev P Y, Korovnikov I V, Skorlotova N A. 2010. To the problem of stage subdivision of the Lower Cambrian. Stratigr Geol Correl, 16: 1–19
Schmitz M D. 2012. Radiogenic isotope geochronology. In: Gradstein F M, Ogg J G, Schmitz M D, Ogg G M, eds. The Geologic Time Scale 2012, vol. 2. Amsterdam: Elsevier BV. 115–126
Shen Y, Schidlowski M. 2000. New C isotope stratigraphy from southwest China: Implications for the placement of the Precambrian-Cambrian boundary on the Yangtze Platform and global correlations. Geology, 28: 623–626
Shields-Zhou G, Zhu M. 2013. Biogeochemical changes across the Ediacaran-Cambrian transition in South China. Precambrian Res, 225: 1–6
Smith E F, Macdonald F A, Petach T A, Bold U, Schrag D P. 2016b. Integrated stratigraphic, geochemical, and paleontological late Ediacaran to early Cambrian records from southwestern Mongolia. Geol Soc Am Bull, 128: 442–468
Smith E F, Nelson L L, Strange M A, Eyster A E, Rowland S M, Schrag D P, Macdonald F A. 2016a. The end of the Ediacaran: Two new exceptionally preserved body fossil assemblages from Mount Dunfee, Nevada, USA. Geology, 44: 911–914
Stein R. 1990. Organic carbon content/sedimentation rate relationship and its paleoenvironmental significance for marine sediments. Geo-Mar Lett, 10: 37–44
Wang D, Ling H F, Struck U, Zhu X K, Zhu M, He T, Yang B, Gamper A, Shields G A. 2018. Coupling of ocean redox and animal evolution during the Ediacaran-Cambrian transition. Nat Commun, 9: 2575
Wang J, Chen D, Yan D, Wei H, Xiang L. 2012. Evolution from an anoxic to oxic deep ocean during the Ediacaran-Cambrian transition and implications for bioradiation. Chem Geol, 306-307: 129–138
Wang X Q, Shi X Y, Jiang G Q, Tang D J. 2014. Organic carbon isotope gradient and ocean stratification across the late Ediacaran-Early Cambrian Yangtze Platform. Sci China Earth Sci, 57: 919–929
Wei G Y, Planavsky N J, Tarhan L G, Chen X, Wei W, Li D, Ling H F. 2018. Marine redox fluctuation as a potential trigger for the Cambrian explosion. Geology, 46: 587–590
Wille M, Nägler T F, Lehmann B, Schröder S, Kramers J D. 2008. Hydrogen sulphide release to surface waters at the Precambrian/Cambrian boundary. Nature, 453: 767–769
Wille M, Nägler T F, Lehmann B, Schröder S, Kramers J D. 2009. Wille et

al. reply. Nature, 459: E6
Wood R A, Poulton S W, Prave A R, Hoffmann K H, Clarkson M O, Guilbaud R, Lyne J W, Tostevin R, Bowyer F, Penny A M, Curtis A, Kasemann S A. 2015. Dynamic redox conditions control late Ediacaran metazoan ecosystems in the Nama Group, Namibia. Precambrian Res, 261: 252–271
Yang C, Zhu M, Condon D J, Li X H. 2017. Geochronological constraints on stratigraphic correlation and oceanic oxygenation in Ediacaran-Cambrian transition in South China. J Asian Earth Sci, 140: 75–81
Yang Y N, Li Q L, Liu Y, Tang G Q, Ling X X, Li X H. 2014. Zircon U-Pb dating by Secondary Ion Mass Spectrometry (in Chinese with English abstract). Earth Sci Front, 21: 81–92
Yao W H, Li Z X, Li W X, Li X H, Yang J H. 2014. From Rodinia to Gondwanaland: A tale of detrital zircon provenance analyses from the southern Nanhua Basin, South China. Am J Sci, 314: 278–313
Zhamoida A I. 2015. General stratigraphic scale of Russia: State of the art and problems. Rus Geol Geophys, 56: 511–523
Zhang J M, Li G X, Zhou C M, Zhu M Y, Yu Z Y. 1997. Carbon isotope profiles and their correlation across the Neoproterozoic-Cambrian boundary interval on the Yangtze Platform, China. Bull Natl Mus Nat Sci, 10: 107–116
Zhang W T, Zhu Z L. 1979. Notes on some trilobites from the Lower Cambrian Houjiashan Formation in southern and southwestern parts of North China (in Chinese with English abstract). Acta Palaeontol Sin, 18: 513–525
Zhou C, Yuan X, Xiao S, Chen Z, Hua H. 2019. Ediacaran integrative stratigraphy and timescale of China. Sci China Earth Sci, 62: 7–24
Zhou M, Luo T, Huff W D, Yang Z, Zhou G, Gan T, Yang H, Zhang D. 2018. Timing the termination of the Doushantuo negative carbon isotope excursion: Evidence from U-Pb ages from the Dengying and Liuchapo formations, South China. Sci Bull, 63: 1431–1438
Zhou M Z, Luo T Y, Liu S R, Qian Z K, Xing L C. 2013. SHRIMP zircon age for a K-bentonite in the top of the Laobao Formation at the Pingyin section, Guizhou, South China. Sci China Earth Sci, 56: 1677–1687
Zhu M Y. 1997. Precambrian-Cambrian Trace Fossils from Eastern Yunnan: Implications for Cambrian Explosion. Bull Natl Mus Nat Sci, 10: 275–312
Zhu M Y, Babcock L E, Peng S C. 2006. Advances in Cambrian stratigraphy and paleontology: Integrating correlation techniques, paleobiology, taphonomy and paleoenvironmental reconstruction. Palaeoworld, 15: 217–222
Zhu M Y, Li G X, Zhang J M, Steiner M, Qian Y, Jiang Z W. 2001. Early Cambrian stratigraphy of East Yunnan, southwestern China: A synthesis. Acta Palaeontol Sin, 40(Suppl): 4–39
Zhu M, Yang A, Yuan J, Li G, Zhang J, Zhao F, Ahn S Y, Miao L. 2019. Cambrian integrative stratigraphy and timescale of China. Sci China Earth Sci, 62: 25–60
Zhu M Y, Yang B, Ahn S Y, Tsukui K, Zhuravlev A Yu, Steiner M, Zhao F C, Ramezani J, Wood R A, Bowring S A. 2017b. Insight into the base of the Cambrian: New data from South China and Siberia. In: McIlroy G, ed. Abstract Volume of the International Symposium on the Ediacaran-Cambrian Transition. 135
Zhu M Y, Zhang J M, Babcock L E, Bowring S A, Ahn S Y, He T C, Yang A H, Li G X, Zhao F C, Yin Z J. 2015. Identification and correlation of the Cambrian base: Problems and potential solutions. In: Gülli E, Piller W E, eds. STRATI 2015, Abstract Ber Inst Erdwiss K-F-Univ Graz, Band 21. 436
Zhu M Y, Zhang J M, Steiner M, Yang A H, Li G X, Erdtmann B D. 2003. Sinian-Cambrian stratigraphic framework for shallow- to deep-water environments of the Yangtze Platform: An integrated approach. Prog Nat Sci, 13: 951–960
Zhu M Y, Zhuravlev A Y, Wood R A, Zhao F C, Sukhov S S. 2017a. A deep root for the Cambrian explosion: Implications of new bio- and chemostratigraphy from the Siberian Platform. Geology, 45: 459–462
Zhu R X, Li X H, Hou X G, Pan Y X, Wang F, Deng C L, He H Y. 2009. SIMS U-Pb zircon age of a tuff layer in the Meishucun section, Yunnan, southwest China: Constraint on the age of the Precambrian-Cambrian boundary. Sci China Ser D-Earth Sci, 52: 1385–1392

(Responsible editor: Maoyan ZHU)